Aerodynamic Loss Characteristics of a Turbine Blade With Trailing Edge Coolant Ejection: Part 1—Effect of Cut-Back Length, Spanwise Rib Spacing, Free-Stream Reynolds Number, and Chordwise Rib Length on Discharge Coefficients

Oguz Uzol

Cengiz Camci
Turbomachinery Heat Transfer Laboratory,
The Pennsylvania State University,
University Park, PA 16802

Boris Glezer
Heat Transfer Team Leader,
Solar Turbines, Inc.,
San Diego, CA 92186

The internal fluid mechanics losses generated between the blade plenum chamber and a reference point located just downstream of the trailing edge are investigated for a turbine blade trailing edge cooling system. The discharge coefficient C_d is presented as a function of the free-stream Reynolds number, cut-back length, spanwise rib spacing, and chordwise rib length. The results are presented in a wide range of coolant to free-stream mass flow rate ratios. The losses from the cooling system show strong free-stream Reynolds number dependency, especially at low ejection rates, when they are correlated against the coolant to free-stream pressure ratio. However, when C_d is correlated against a coolant to free-stream mass flow rate ratio, the Reynolds number dependency is eliminated. The current data clearly show that internal viscous losses due to varying rib lengths do not differ significantly. The interaction of the external wall jet in the cutback region with the free-stream fluid is also a strong contributor to the losses. Since the discharge coefficients do not have Reynolds number dependency at high ejection rates, C_d experiments can be performed at a low free-stream Reynolds number. Running a discharge coefficient experiment at low Reynolds number (or even in still air) will sufficiently define the high blowing rate portion of the curve. This approach is extremely time efficient and economical in finding the worst possible C_d value for a given trailing edge coolant system.
[DOI: 10.1115/1.1348017]

Introduction

The current project deals with an investigation of aerodynamic discharge coefficients obtained for the trailing edge coolant ejection system of a turbine blade. Due to increasing turbine inlet temperatures, internal and external cooling of turbine nozzle vanes and rotor blades including trailing edge ejection is becoming increasingly popular in modern systems. Improvements of 3–5 percent in direct operating cost and 8–10 percent in fuel efficiency of future gas turbine engines are possible. There are currently at least three major reasons for continued strong interest in turbine cooling research. According to Metzger et al. [1], ''the first and the foremost reason is the enormous turbine inlet temperature potential of around 2000 °C (3700 °F) set by stoichiometric combustion and the fact that use of higher temperatures (and corresponding higher pressure ratios) improves performance.'' Second is the underlying nature of both hot gas and coolant flows as highly turbulent, unsteady, three-dimensional, and geometry-dependent flows that have not yet yielded to general solutions. Third, although new aerodynamic advances and new manufacturing techniques generate new conceptual changes, their time-efficient analysis and design implementation are still in their infancy. Despite well-publicized advances in material capability, the current maximum allowable component metal temperatures are still only about 1000 °C (1800 °F). The current maximum turbine inlet temperatures are presently around 1450 °C (2600 °F). The difference of 800 °F has been primarily achieved through dramatic improvements in turbine cooling methods. Although the initial idea of an uncooled transonic turbine passage is very attractive because of the elimination of coolant ejection related aerodynamic penalties, the current level of maximum allowable metal temperatures clearly eliminates this approach. Our continued benefit from elevated inlet temperatures is only possible by effectively using cooling systems internally and externally. Understanding the internal flow physics due to trailing edge coolant ejection in turbine passages and generating an applicable and reliable set of discharge coefficient distributions is the main goal of this paper.

Related Past Studies

Several past investigators have studied the influence of coolant ejection on aerodynamic losses in turbine passages, including McMartin and Norbury [2], Prust [3], Lokai and Kumirov [4], Lawaczek [5], and Sturedus [6]. General observations indicate that different ejection geometries were used by different investigators with varying experimental uncertainty levels and their results are

Contributed by the International Gas Turbine Institute and presented at the 45th International Gas Turbine and Aeroengine Congress and Exhibition, Munich, Germany, May 8–11, 2000. Manuscript received by the International Gas Turbine Institute February 2000. Paper No. 2000-GT-258. Review Chair: D. Ballal.

somewhat inconclusive. A general trend was the excessive use of relatively thick trailing edges. A consistent set of discharge coefficients evaluated as a function of coolant to free-stream ejection rate, cutback length, free-stream Reynolds number, and rib geometry used inside the trailing edge does not exist.

Aerodynamic losses due to pressure side coolant ejection in a transonic turbine cascade are described by Moses et al. [7]. Although the ejection is on the pressure side of the blade, their configuration can best be described as trailing edge ejection system discharging near the pressure side. Only aerodynamic results are presented for an exit Mach number range of 0.7–1.4. Their results for the blowing rate range from 0 to 1.7 showed that there was little effect of the coolant ejection on the flow field and on the aerodynamic losses. Their conclusion was consistent with that of Venediktov [8] who used similar geometry and blowing conditions. Coolant ejection into local supersonic flow strongly influences the aerodynamic losses in a turbine, Kiock et al. [9]. Three rows of holes near the leading edge and a trailing edge ejection system were considered. They observed that the roughness due to the ejection holes near the leading edge did not influence the blade boundary layer behavior. However, local ejection near the leading edge and near the throat affects the transition. Typical ejections near the suction side throat almost doubles the momentum thickness near the trailing edge. Part of the wake is filled with trailing edge cooling jets so that the energy content in the exit plane increases with increasing coolant flow rate and can exceed the mainstream energy level at the inlet. The aerodynamic mixing effect of discrete cooling jets with mainstream flow on a highly loaded turbine blade is presented in Wilfert and Fottner [10]. A single row of holes located at 40 percent chord on the suction side is studied. The hole spacing is about 2.5 times that of the hole diameter. The maximum free-stream turbulence level was about 6.5 percent. The aerodynamic losses showed a minimum at a blowing rate of 1.5.

Experimental Facility

The experiments are conducted at the ''Cooled Turbine Cascade Facility'' at the Turbomachinery Heat Transfer Laboratory of the Pennsylvania State University. This is an open-loop wind tunnel that consists of an axial air blower, a diffuser with multiple screens, a plenum chamber, a high area ratio circular nozzle, a circular to rectangular transition duct, and the test section. The schematic of the facility is shown in Fig. 1. The air blower is a 45.7 cm tip diameter fan which is driven by a 7.5 kW electric motor. The fan has a potential to provide a pressure differential of 15 cm of water over a range of flow rates. The speed of the electric motor is controlled by an adjustable frequency AC drive, which gives the ability to control the air speed through the facility.

The three-bladed linear turbine cascade used in the present study is shown in Fig. 2. The original design of the blade profile, the cascade arrangement, and the typical velocity distribution around the airfoil is described in Gaugler and Russel [11] and

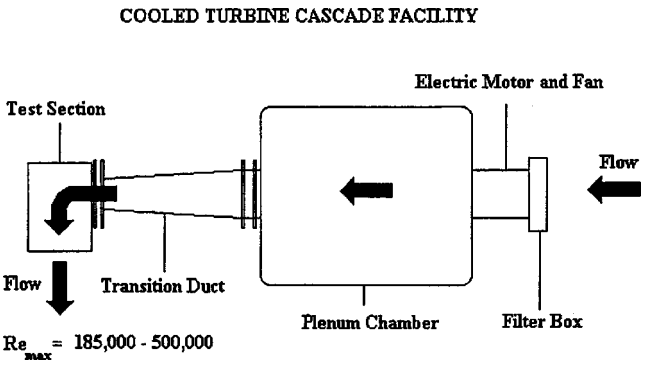

Fig. 1 Experimental facility

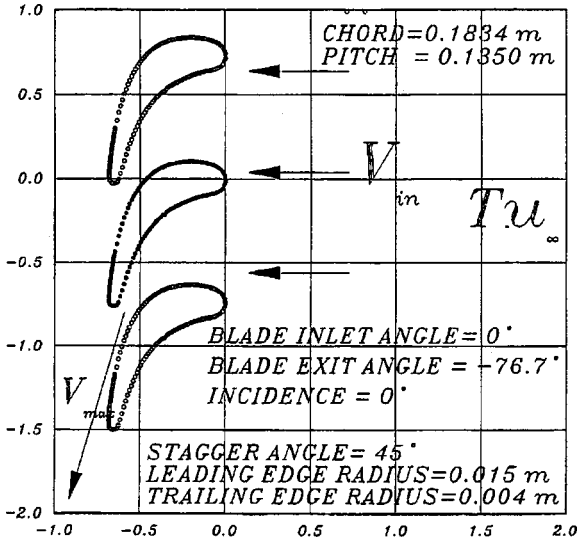

Fig. 2 Linear turbine cascade

Hippensteele et al. [12]. The chord length of the blades precision machined from wood is 0.1834 m and the pitch–chord ratio is 0.736. The blade inlet angle is 0 deg and blade exit angle is −76.7 deg. All experiments reported in this paper are performed at zero incidence. The cascade arrangement has a stagger angle of 45 deg. Since specific attention is paid to the flow physics near the cooled trailing edge section, the geometric details of the trailing edge area and the throat section of the turbine passage are shown in Fig. 3. The maximum velocity V_{max} at the exit of the cascade has been measured near the center of the throat circle. The location of the maximum velocity between the pressure side and the suction side has also been confirmed by Particle Image Velocimeter (PIV) measurements, described in Uzol and Camci [13].

A pressure side view of the trailing edge cooling system and the copper coolant feeding pipe is shown in Fig. 4. The metered coolant is fed into the system from both sides of the pipe. The copper pipe has 13 oblong openings, providing an effective area of 300.8 mm^2. The internal cavity of the cooling passage shown in Fig. 4 (without any ribs installed) is machined in a numerically con-

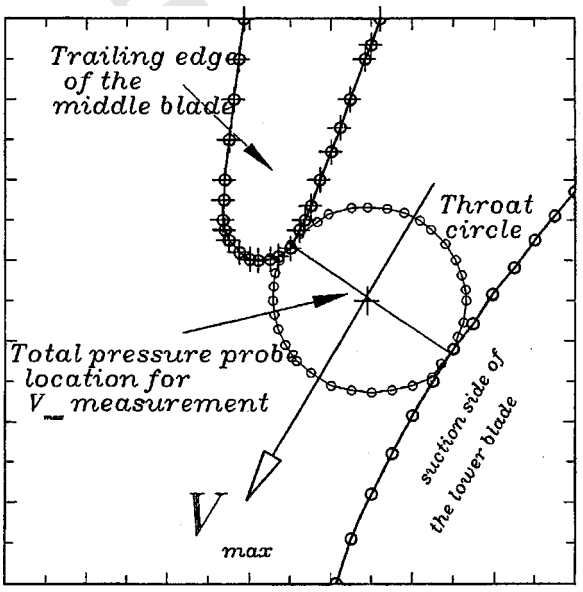

Fig. 3 Trailing edge details and throat section

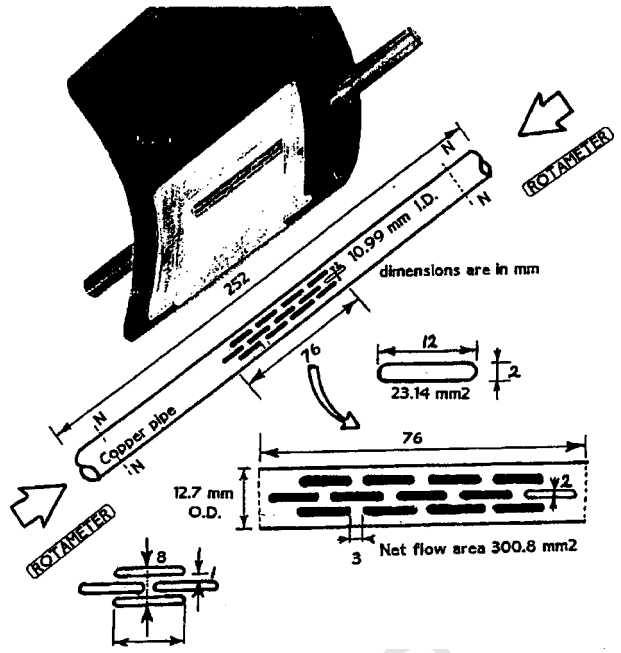

Fig. 4 Trailing edge cooling system and plenum chamber details

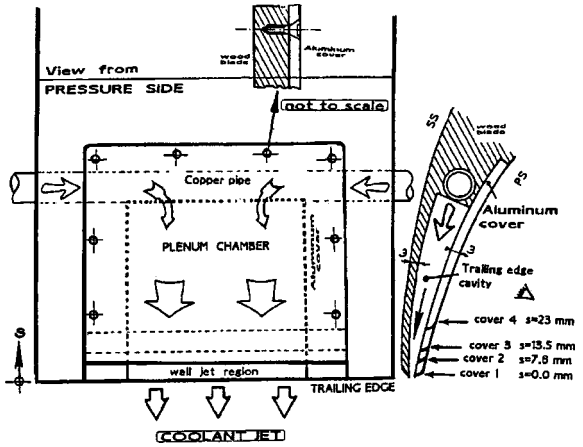

Fig. 5 Cut-back configurations and the trailing edge cavity

trolled milling machine. Special emphasis is paid to maintain a spanwise uniformity of coolant air downstream of the 13 holes. Four different aluminum covers carefully shaped to the original profile of the pressure side provide four different cut-back lengths used throughout the study.

Figure 5 presents the four individual cut-back configurations and the overall geometry of the trailing edge cavity without any ribs installed. The geometry of the wall jet region that occupies the region between the lip of the pressure side cover and the trailing edge point is extremely important because of its tremendous contribution to the final formation of the wake flow containing coolant fluid. This contribution is evident in the present computations explained in Part 2 [13]. It is apparent that the overall wake width controlling the total pressure losses can be reduced by carefully designing the cut-back trailing edge geometry on the pressure side. Figure 6 describes four different cut-back pressure side configurations obtained by altering the aluminum pressure side cover. Channel height h at the exit location is described in Fig. 6 for each cut-back length used in the study.

Figure 7 summarizes the three different rib configurations mounted inside the trailing edge cavity. Model *A* has the largest

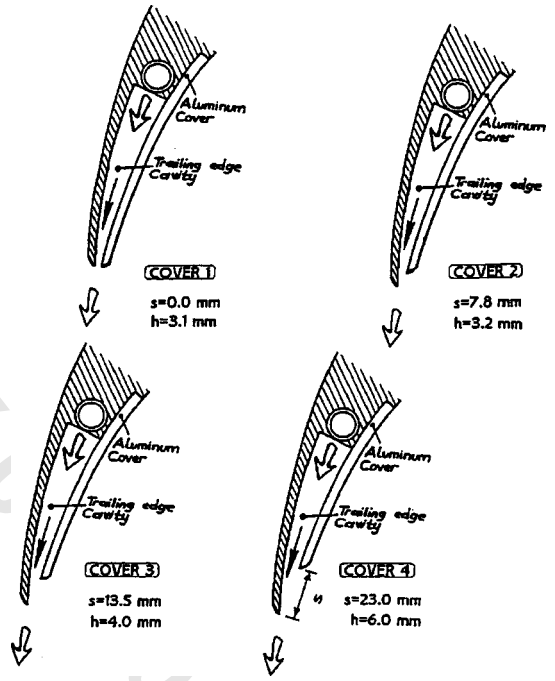

Fig. 6 Four different cut-back lengths

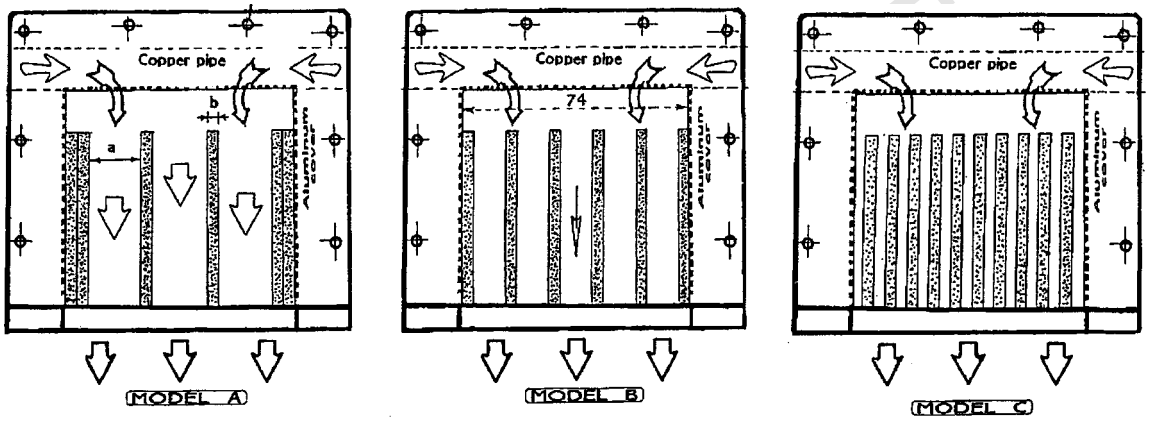

Fig. 7 Three different rib arrangements (Models *A*, *B*, *C*)

Table 1 Rib arrangement data (Models A, B, C)

MODEL A	COVER 1 h=3.1 mm	COVER 2 h=3.2 mm	COVER 3 h=4 mm	COVER 4 h=6 mm
Rib width in spanwise direction b=3.17 mm	b/h=1.02	b/h=0.99	b/h=0.79	b/h=0.53
Rib spacing in spanwise direction a=18.5 mm	a/h=5.97	a/h=5.78	a/h=4.62	a/h=3.08
Effective exit flow area A_{ex} (mm^2)	172	178	222	333

MODEL B	COVER 1 h=3.1 mm	COVER 2 h=3.2 mm	COVER 3 h=4 mm	COVER 4 h=6 mm
Rib width in spanwise direction b=3.17 mm	b/h=1.02	b/h=0.99	b/h=0.79	b/h=0.53
Rib spacing in spanwise direction a=10.88 mm	a/h=3.51	a/h=3.40	a/h=2.72	a/h=1.81
Effective exit flow area A_{ex} (mm^2)	169	174	218	326

MODEL C	COVER 1 h=3.1 mm	COVER 2 h=3.2 mm	COVER 3 h=4 mm	COVER 4 h=6 mm
Rib width in spanwise direction b=3.17 mm	b/h=1.02	b/h=0.99	b/h=0.79	b/h=0.53
Rib spacing in spanwise direction a=4.55 mm	a/h=1.47	a/h=1.42	a/h=1.14	a/h=0.76
Effective exit flow area A_{ex} (mm^2)	127	131	164	246

spanwise rib spacing of $a=18.5$ mm in a three-channel configuration. Spanwise rib width for all three cases is the same at $b=3.17$ mm. Although all three configurations in Fig. 7 are shown with ''Cover 2,'' the effective exit flow areas evaluated at the pressure side lip point for ''Cover 1,'' ''Cover 3,'' ''Cover 4'' (Fig. 6) are numerically tabulated in Table 1 and ''h'' is defined as the distance between the suction side shell and the pressure side shell at the cut-back lip location. ''Model B'' and ''Model C'' have 5 and 11 channels, respectively.

Discharge Coefficient Measurements

The free-stream total and static pressures are measured at the inlet of the test section using a Pitot probe by recording the outputs of the probe through separate channels. The total temperature of the free stream is measured using a thermistor based temperature sensor. In addition to free stream measurements, the maximum velocity inside the passage is also measured at the minimum area location (throat) between the pressure side of the middle blade and the suction side of the lower blade using a Pitot probe (Fig. 3).

The discharge coefficient for the trailing edge cooling system can be defined as the ratio of the actual mass flux rate to the isentropic mass flux rate that is the maximum possible value for one-dimensional flow. Therefore,

$$C_d=(\rho_c u_c)_{\text{act}}/(\rho_c u_c)_{is} \tag{1}$$

The actual mass flux rate is calculated using the measured coolant mass flow rate $\dot{m}_{\text{act}}$ and the exit area A_{ex} at the end of the trailing edge coolant cavity. The point at which A_{ex} is calculated for each of the four different cut-back lengths coincides with the lip of the pressure side as shown in Fig. 5. The actual coolant mass flux rate can then be calculated as,

$$(\rho_c u_c)_{\text{act}}=\dot{m}_{\text{act}}/A_{ex} \tag{2}$$

The isentropic mass flux rate can be calculated from one-dimensional momentum equation and the equation of state for air,

$$(\rho_c u_c)_{is}=P_{c_{ex}}\left(\frac{P_{t_c}}{P_{c_{ex}}}\right)^{(\gamma-1)/\gamma}\cdot\left\{\frac{2\gamma}{\gamma-1}\cdot\frac{1}{RT_{t_c}}\times\left[1-\left(\frac{P_{t_c}}{P_{c_{ex}}}\right)^{(\gamma-1)/\gamma}\right]\right\}^{1/2} \tag{3}$$

Equation (3) provides the maximum possible flux rate of coolant air between a coolant total pressure of P_{tc} and the coolant exit static P. The exit static pressure in the coolant stream is measured at 3 mm downstream of the trailing edge point of the blade using a 1.8-mm-dia Pitot-Static probe. The coolant total pressure P and coolant static pressure P_c are measured inside the copper pipe at section N–N as shown in Fig. 4. The copper plenum chamber is fed by two air supply pipes that have individual precision rotameters for volumetric flow rate measurements. The density of air at the rotameter location is calculated from the measured temperature and pressure values at the metering stations. Effective passage exit area A_{ex} for each configuration is measured at the pressure side lip location for each cut-back length and rib configuration. Twelve individual A_{ex} values obtained from three rib spacings and four different cutback lengths are tabulated in Table 1. The experimental uncertainties on the different measured quantities have been estimated as follows, based on a 20:1 confidence interval:

$\delta p=\pm 0.5$ percent at $p=105{,}000$ N/m^2 (typical atmospheric value)
$\delta T=\pm 0.2$ percent at $T=300$ K (typical inlet value)
$\delta\dot{m}_c=\pm 1.2$ percent at $\dot{m}_c=0.005$ kg/s
$\delta(\dot{m}_c/\dot{m}_\infty)=\pm 1.6$ percent at $(\dot{m}_c/\dot{m}_\infty)=0.02$
$\delta C_d=\pm 2.8$ percent at $C_d=0.60$

Experimental Results and Discussion

Table 2 summarizes the free-stream flow conditions during the experiments performed at three different Reynolds numbers defined by the true chord and exit velocity ($V_{ex}=V_{\max}$). Low, medium, and high Reynolds numbers based on exit velocity were 185,701, 358,029, and 505,868, respectively. The coolant ejection experiments were also performed in the absence of free-stream flow as a reference case. Free-stream turbulence intensity was kept at approximately $Tu_\infty=1.2$ percent for all experiments.

Discharge Coefficients (Model *A*). Figures 8–10 show the variation of discharge coefficients against the coolant to free-stream static pressure ratio P_{tc}/P_{cex}. The second column in each figure presents C_d data against coolant to free-stream mass flow rate ratio for Models *A*, *B*, and *C*. The three models represent three different rib spacings as described in Fig. 7. Four different cut-back lengths for each model are simulated by four different individual pressure side covers as shown in Fig. 6. A wide coolant to free-stream mass flow rate range from 0 to 5 percent is used in experiments. This range is sufficient to cover most gas turbine trailing edge cooling applications.

The results from the three models show that there is always a threshold coolant pressure above which the discharge coefficients do not have any free-stream Reynolds number dependency. For Covers 1, 2, and 3, this threshold level is about $P_{tc}/P_{cex}=1.003$. This threshold value is around 1.010 when Cover 4 is used. The flow losses in the trailing edge cavity are Reynolds

Table 2 Typical free-stream flow conditions at the cascade inlet and exit (exit is defined as the maximum velocity pint at the throat area and Reynolds numbers are based on true chord lenth)

		INLET VELOCITY V_{inlet}	INLET REYNOLDS NUMBER Re_{inlet}	EXIT VELOCITY V_{exit}	EXIT REYNOLDS NUMBER Re_{exit}	SYMBOL
		m/s		m/s		
HIGH REYNOLDS NUMBER	Re_H	7.8	90334	44.1	505868	△
MEDIUM REYNOLDS NUMBER	Re_M	4.7	55187	30.9	358029	○
LOW REYNOLDS NUMBER	Re_L	1.9	21607	16.1	185701	▼
NO MAINSTREAM FLOW	Re_O	0	0	0	0	+

number dependent in the low P_{tc}/P_{cex} range shown in the figures. The effective exit area of the trailing cooling cavity is the largest when Cover 4 is used.

The dependency of the discharge coefficient data on the coolant to free-stream pressure ratio can easily be removed by plotting C_d against coolant to free-stream mass flow rate ratio instead of the pressure ratio. The independence of C_d from Reynolds number for this case is regardless of the rib spacing ''*a*'' or the cut-back length ''*s*'' used in the experiments summarized in Figs. 8–10. One explanation for this observation may be the strong functional dependency of the coolant mass flux rate to the coolant to free-stream pressure ratio P_{tc}/P_{cex} as described in Eq. (3). For small coolant to free-stream pressure ratio values at which this functional dependency is strong, a high level of dependency of C_d to pressure ratio is observed. Using mass flow rate ratio also stretches the horizontal axis.

The data presented in Figs. 8–10 show the no-free-stream flow case as a reference case. In all plots, a plus sign is assigned to no-free-stream flow experiments in which coolant jet issued from the trailing edge directly ejects into still air at atmospheric pressure. Covers 1, 2, and 3 produces the lowest C_d coefficients when

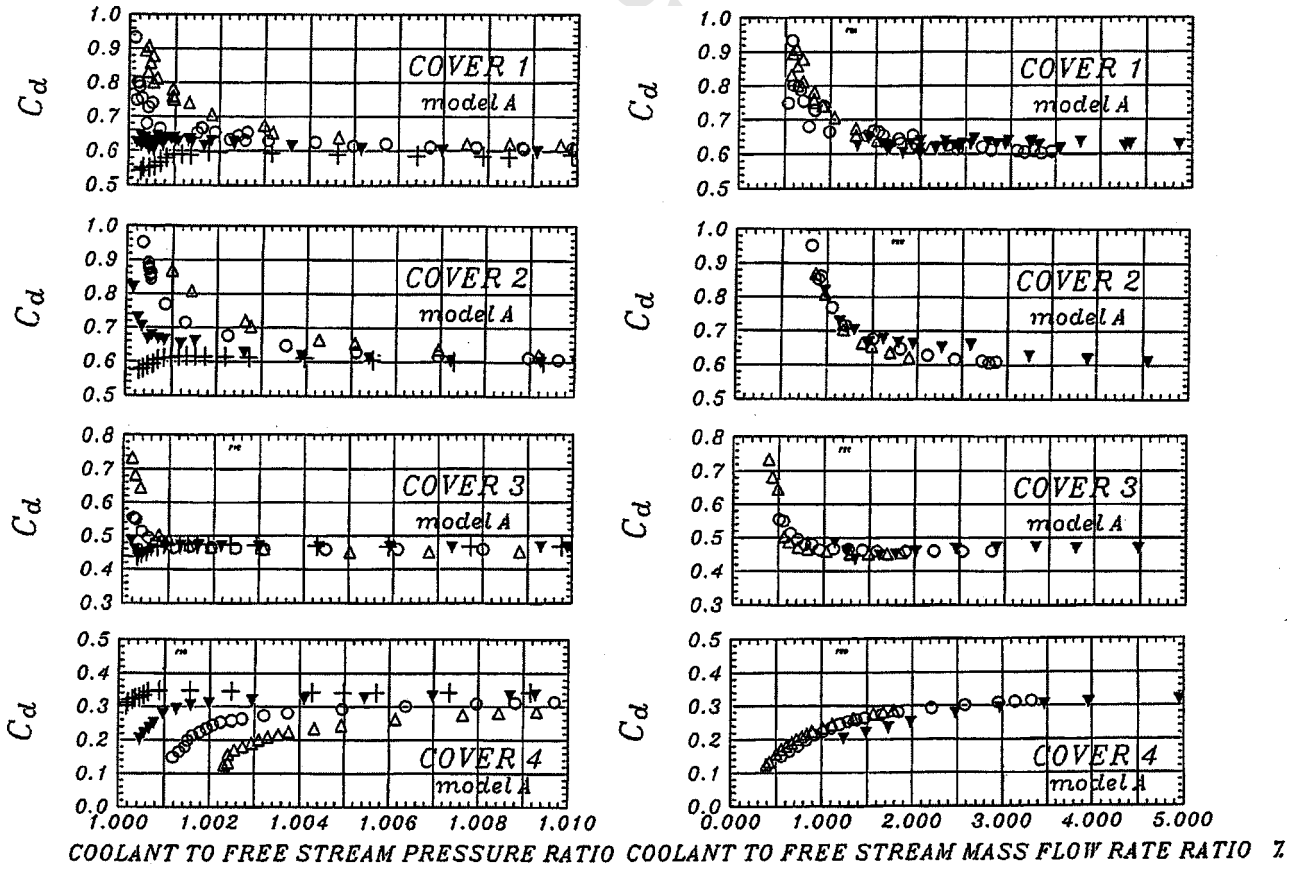

Fig. 8 Discharge coefficients for Model *A*

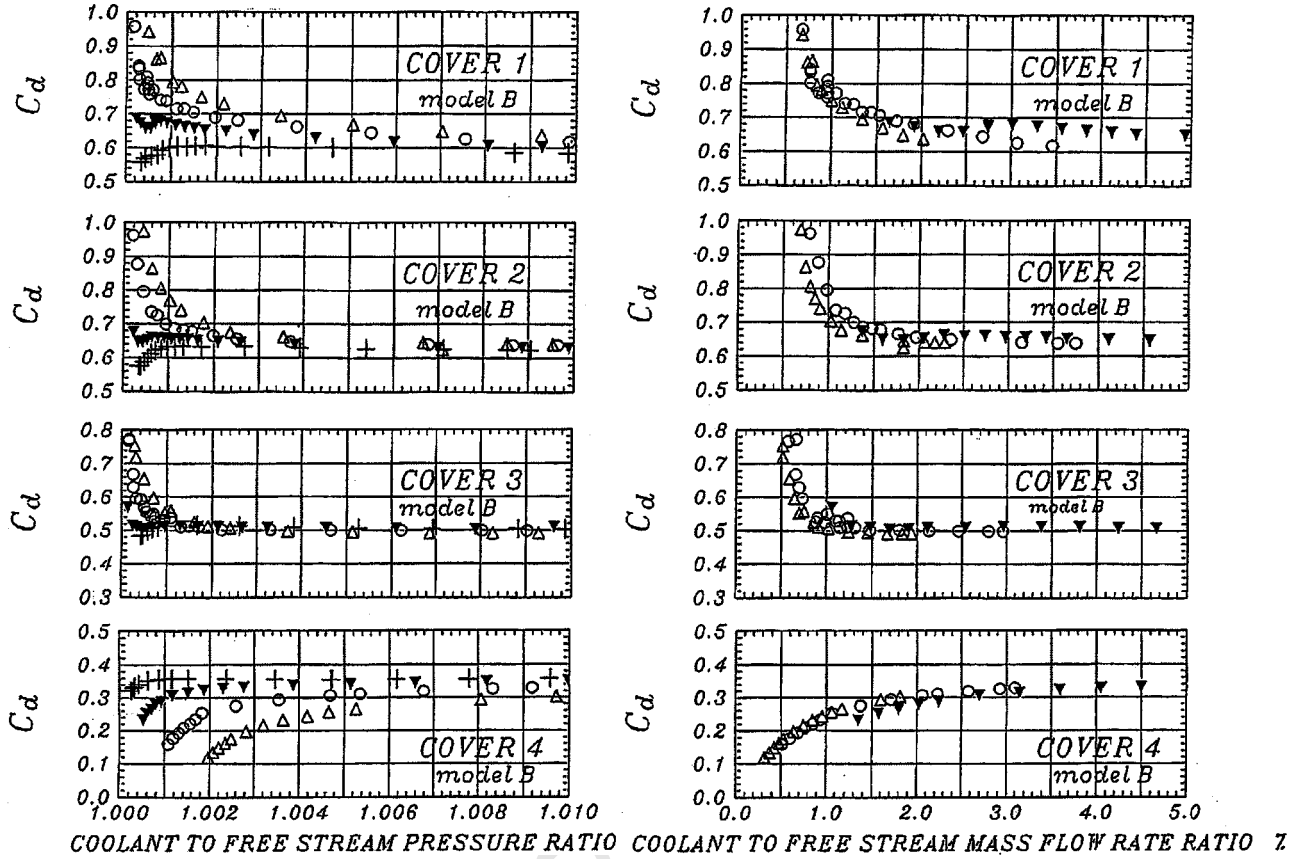

Fig. 9 Discharge coefficients for model *B*

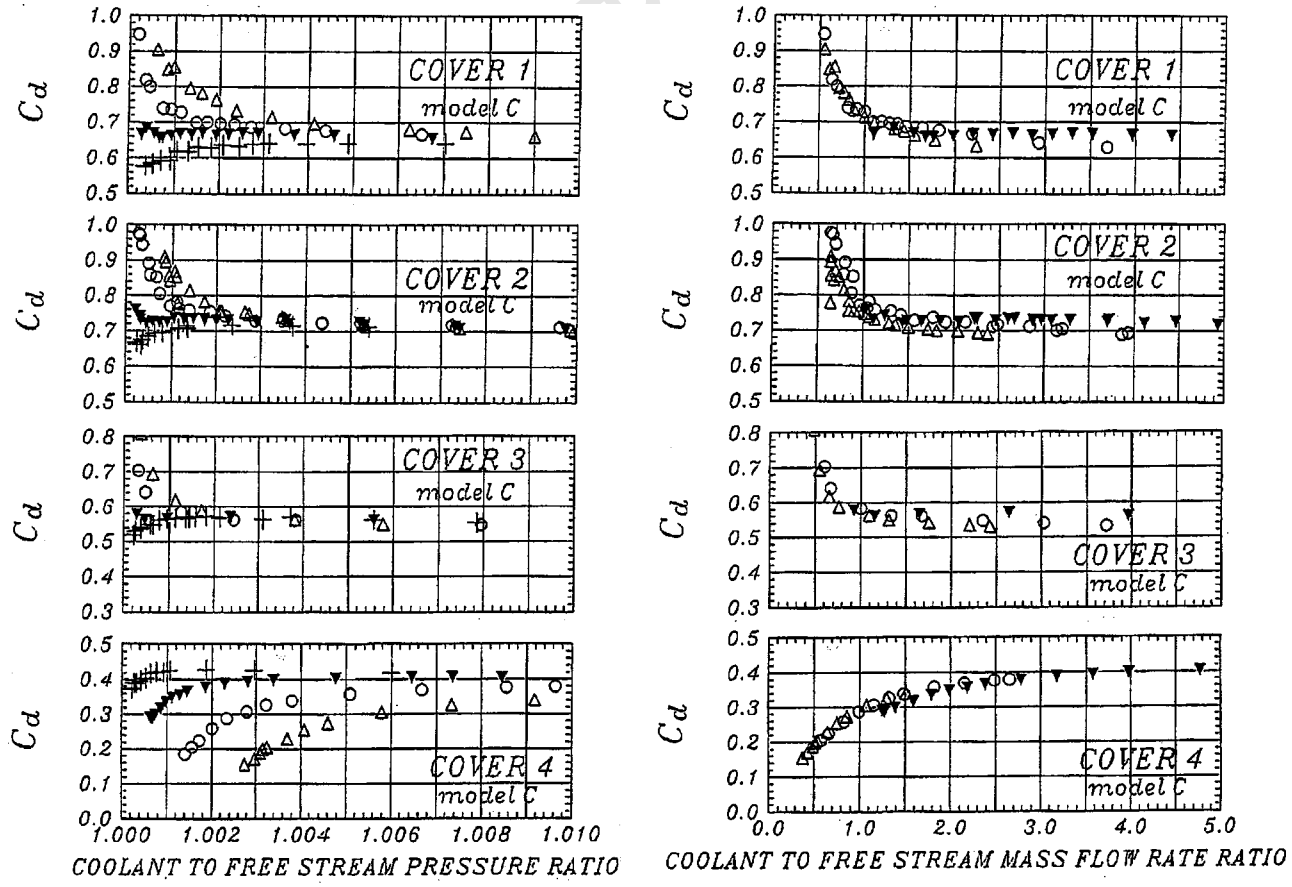

Fig. 10 Discharge coefficients for model *C*

the pressure ratio is less than the previously mentioned threshold level of approximately $P_{tc}/P_{cex}=1.003$. For this case, the exit pressure is atmospheric in still air and relatively higher than the exit pressure levels imposed by the ''low,'' ''medium,'' and ''high'' Reynolds number experiments.

In general, the discharge coefficients from ''Cover 4,'' which has the longest cut-back length, have the lowest values. This observation could be attributed to the fact that the effective exit area measured at the pressure side lip is the largest (when compared to other shorter cut-back lengths). The larger exit area results in a relatively low momentum wall jet near the trailing edge. Since the downstream pressure probe is located about 3 mm downstream of the trailing edge point, the C_d values measured in this study naturally include the losses in the trailing edge cavity and in the wall jet located between the pressure side lip and the probe location. The wall jet is bounded by the suction side shell of the blade on one side; however, the free shear layer existing between the free-stream and the wall jet is a major aerodynamic loss generation element in this configuration. The relatively low momentum coolant jet character imposed by the largest ($h=6$ mm) exit area creates a ''loss prone'' wall jet. For covers 1, 2, and 3, decreasing the coolant to free-stream pressure ratio causes an increase in the discharge coefficient. However, for Cover 4 this causes a decrease in the discharge coefficient, which indicates more losses are created. This change in the character of the loss generation mechanism is mainly due to the formation of a strong recirculatory flow inside the cut-back region for low ejection rates, as the cut-back length increases. As the ejection rate is increased, the recirculatory flow disappears and the ejected coolant flow starts to dominate the cut-back region. Hence, the discharge coefficient values are less influenced by this effect. The formation and the disappearance of the recirculatory region inside the cut-back length are visualized with the computational simulations discussed in Uzol and Camci [13]. Consequently the low momentum wall jet guided by the suction side shell makes ''Cover 4'' (or the longest cut-back length case) the least ideal case as far as the discharge coefficients are concerned.

Figures 8–10 clearly show that the discharge coefficients are continually improved below the threshold coolant pressure when the free-stream Reynolds number is gradually increased, from zero to low, medium, and high values for Covers 1, 2, and 3. Varying the Reynolds number at a constant coolant pressure ratio of P_{tc}/P_{cex}, only affects the losses in the wall jet region because at each Reynolds number case the free-stream velocity at the edge of the free shear layer is different. The shear-generating velocity difference between the wall jet and the free-stream flow is the main contributor to the loss generation. The discharge coefficient assumes its lowest value when the coolant is ejected into still air. The shear generated in the wall jet region of the coolant stream is maximum for this case because of the maximum possible velocity differential between the coolant and the free-stream flow.

When Cover 4, which has the longest cut-back length, is installed, the momentum of the wall jet issued at the exit plane (pressure side lip) is extremely low due to the large effective exit area ($h=6$ mm). Figures 8–10 show extremely low values of C_d for the cooling system because of the interaction of a low momentum (possibly laminar coolant jet) with the free-stream flow. For this case, increasing the free-stream Reynolds number does not improve the discharge coefficients. The losses become larger as the free-stream Reynolds number is increased at a fixed coolant pressure.

A plot of the $C_d$values against the ''coolant to free-stream pressure ratio'' is extremely illuminating to understand the contribution of free-stream to aerodynamic losses of a trailing edge cooling system. When the coolant pressure is gradually increased at a fixed free-stream Reynolds number, a practically constant C_d value is reached quickly. For example, for Covers 1, 2, and 3, when P_{tc}/P_{cex} values are greater than 1.003, further increases in the plenum chamber pressure does not affect the overall aerodynamic losses. A nearly constant C_d value for high blowing rates is about 0.61 for Cover 1, Fig. 8. Cover 2 has slightly higher loss, possibly because of the relatively shorter wall-jet region that exists for this model. Once the coolant jet reaches a momentum level equal to or higher than that of the free stream, further increases in the coolant pressure do not influence the losses in a significant manner. The nearly constant value of C_d is determined by the internal fluid mechanic features of the trailing edge cavity but not by the wall jet contributions occurring outside trailing edge cavity. However, in the given coolant mass flow range, the influence of varying coolant pressure is not significant as far as the final level of C_d is concerned. The main reason for the nearly constant C_d level could be attributed to the fact that once the coolant jet reaches a certain momentum level, the free-stream flow cannot easily modify the jet. The main loss contributing parameters of the cavity may be the overall volume of the cavity, the effective exit area, the open friction area defined by the ribs, and the free-stream static pressure at the pressure side lip location.

The aerodynamic losses are at the same level when the discharge coefficient C_d is evaluated for various free-stream Reynolds numbers at the same coolant to free-stream mass flow ratio. The independence from the Reynolds number is because the relative velocity ratios between the free stream and coolant jet are kept the same when the coolant mass flow rate ratio is employed as the horizontal axis. When the coolant to free-stream mass flow rate ratios are the same, the coolant to free-stream pressure ratios assigned to each free-stream Reynolds number experiment are naturally different. The second column in Figs. 8–10 contains C_d data as functions of the coolant to free-stream mass flow rate ratio. The observed collapsing character of various C_d distributions obtained in a wide free-stream Reynolds number range is an extremely useful property for the cooling designer. In a wide free-stream Reynolds number range from 185,701 to 505,868, the discharge coefficients show minimal Reynolds number dependency, which is well within the experimental measurement error on discharge coefficient ($\delta C_d=\pm 2.8$ percent).

Discharge Coefficients (Model *B*). Similar results are observed for Model *B*, which has a closer rib spacing ($a=10.88$ mm) with five distinct internal flow channels, as described in Fig. 7. Although the net flow friction area is increased by the addition of two more ribs, it is likely that the fluid mechanic losses in each of the five channels are reduced when compared to model *A*. The effective exit area value for each of the covers is also slightly reduced because of rib addition when compared to Model *A*. The discharge coefficient values obtained for high blowing rates for Model *B* are about 7 percent higher than those of Model *A* (on average) for all four cut-back lengths, as shown in Fig. 9.

Discharge Coefficients (Model *C*). Figure 10 presents the discharge coefficients from Model *C* for a ten-ribbed internal configuration that has 11 individual flow passages. Although the cavity friction area is increased significantly (about 25 percent compared to Model *A*), the overall losses are reduced. The effective exit area is reduced by about 26 percent, resulting in a higher momentum coolant jet at the pressure side lip. The measured discharge coefficients are about 15 percent higher on the average for Model *C* when compared to Model *A*. The increased rib spacing used in Model *C* results in the best overall discharge coefficient over a wide coolant mass flow rate range.

Low Re Experiments and the Worst Case Discharge Coefficients. The data presented in Figs. 8–10 suggest that discharge coefficients for a cooled trailing edge system with a cut-back length can be obtained from experiments performed at low Reynolds numbers without sacrificing accuracy. This approach eliminates the requirement of operating a test facility at full Reynolds number. Tremendous energy and time savings can be obtained from the acquisition of C_d data in low Reynolds number experiments. A very quick estimate of the trailing edge cooling system

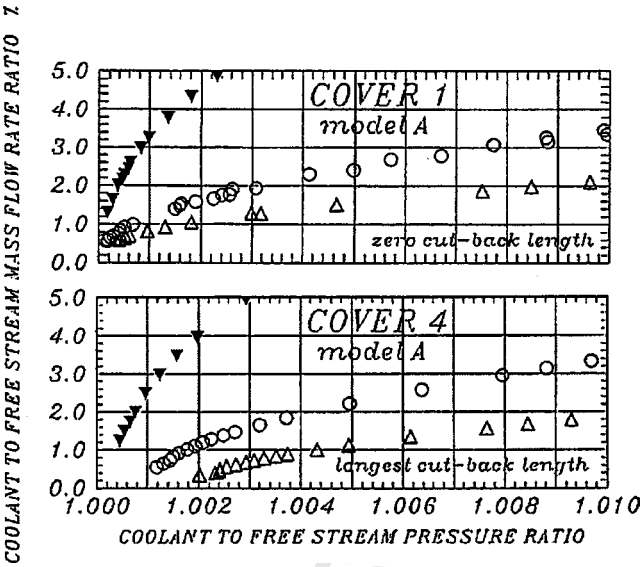

Fig. 11 Actual coolant mass flow rate ratio versus pressure ratio (model *A*, Covers 1 and 4)

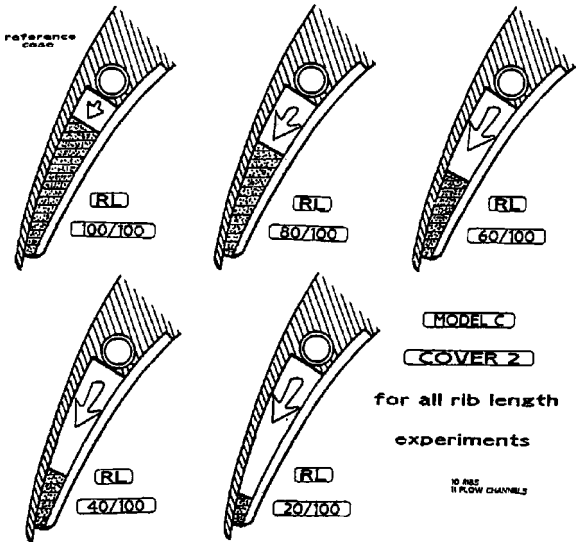

Fig. 12 Five different rib lengths (Model *C*, Cover 2)

performance can even be obtained by simply running the C_d experiment at zero free-stream Reynolds number. This approach can be realized even outside the test section of a wind tunnel by just ejecting the cooling air into still air. All experiments performed in still air shown in Figs. 8–10 with many rib spacings and cut-back lengths clearly show that the zero Reynolds number discharge coefficients (as shown by + signs) always merge to actual Reynolds number results when the threshold coolant to free-stream pressure level is exceeded. If the horizontal axis is chosen as the ''coolant to free-stream mass flow rate ratio,'' any experiment over $\dot{m}_c/\dot{m}_\infty = 2.5$ percent produces the asymptotic value of C_d that may be used as a worst-case discharge coefficient estimate. The trailing edge ejection system with Covers 1, 2, and 3 cannot perform worse than this asymptotic value. The system may actually perform much better than this limiting value at low coolant mass flow rate ratio values that are less than 1 percent.

Coolant Mass Flow Versus Pressure Ratio. Figure 11 shows the capability of Model *A* to pass coolant mass flow rate for a given coolant to free-stream pressure ratio. The results for the shortest cutback length (Cover 1, $s = 0.0$ mm) and the longest cut-back length (Cover 4, $s = 23.0$ mm) indicate that a shortening of the cut-back region length improves the coolant mass flow rate passing capability of the ejection system at a fixed pressure ratio. When the shortest cutback length data shows a 5 percent coolant mass flow rate ratio at a coolant mass flow ratio of 4.2 percent. This reduction is related to the additional shear layer related losses generated in the wall jet section. When the same experiment is repeated with the same cover and rib configuration (Cover 1, Model *A*) for different free-stream Reynolds numbers, the low Reynolds number experiment provides the highest coolant mass flow rate at a fixed P_{tc}/P_{cex}. The highest Reynolds number experiment results in the lowest coolant mass flow rate ratio at the same coolant pressure ratio. Since the ratio P_{tc}/P_{cex} is kept constant, the relatively low free-stream static pressure of the high free-stream Reynolds number experiment require a lower coolant pressure than the low Reynolds number experiment. During a high free-stream Reynolds number experiment, the coolant pressure needs to be reduced in order to keep the pressure ratio the same.

Influence of Rib Length on Discharge Coefficients. The viscous flow losses in the trailing edge cavity need to be quantified for the length of the ribs used inside the cooling system. The rib length experiments performed in this study use the most successful aerodynamic configuration as far as the rib spacing and cut-back length is concerned. Figure 12 presents five different relative rib lengths ranging from 20 to 100 percent using Cover 2 and Model *C*. The corresponding cut-back length is fixed at 7.8 mm. The rib spacing is 4.55 mm with 11 flow channels. There are two major parameters to be considered in discussing the influence of rib length on the discharge coefficients: the specific three-dimensional flow in the chamber between the coolant pipe and the rib and the flow between the ribs described in Fig. 12.

Figure 13 presents measured discharge coefficients obtained from five different rib lengths at two different free-stream Reynolds numbers. The experimental results with no free-stream flow are also included. An immediate observation made from Fig. 13 is that varying rib length does not significantly affect the discharge coefficients for a constant free-stream Reynolds number. In all three experiments performed at different Reynolds numbers, the longer rib configurations result in slightly lower C_d values. However, when the data from all five rib lengths are plotted together, the maximum variation in the discharge coefficient values are less than ± 1.5 percent on C_d, Fig. 14. When low and high free-stream Reynolds number C_d data for all five rib lengths are plotted against the coolant to free-stream mass flow rate ratio, it can be concluded that the influence of rib length on the discharge coefficient of the trailing edge cooling systems considered is not significant. Figure 14 indicates that the discharge coefficient variation with respect to coolant mass flow rate ratio is only significant when the coolant flow rate ratio is less than 1.5 percent. Above 1.5 percent, the C_d has a constant value that can be taken as the worst possible discharge coefficient that can be assigned to a given cooling system. Figure 14 is an independent confirmation of the similar results presented in Figs. 8–10. All of the experiments performed in this study show that the nearly constant C_d value from the high blowing rate experiments can be accurately obtained from a zero free-stream Reynolds number experiment setup with a cooled blade discharging into still air.

The coolant mass flow rate passing capability of the trailing edge cooling system with five different rib lengths is shown in Fig. 15. The results obtained for low and high Reynolds numbers show no rib-length dependency in a wide coolant to free-stream pressure ratio range.

Spanwise Uniformity Tests. Spanwise uniformity of the coolant ejection at the trailing edge is checked by traversing along the spanwise direction 20 mm downstream of the trailing edge. Model *B* with Cover 2 is used for the test and a kiel probe with a 3.175 mm shield diameter is used for the traverse. The tests are

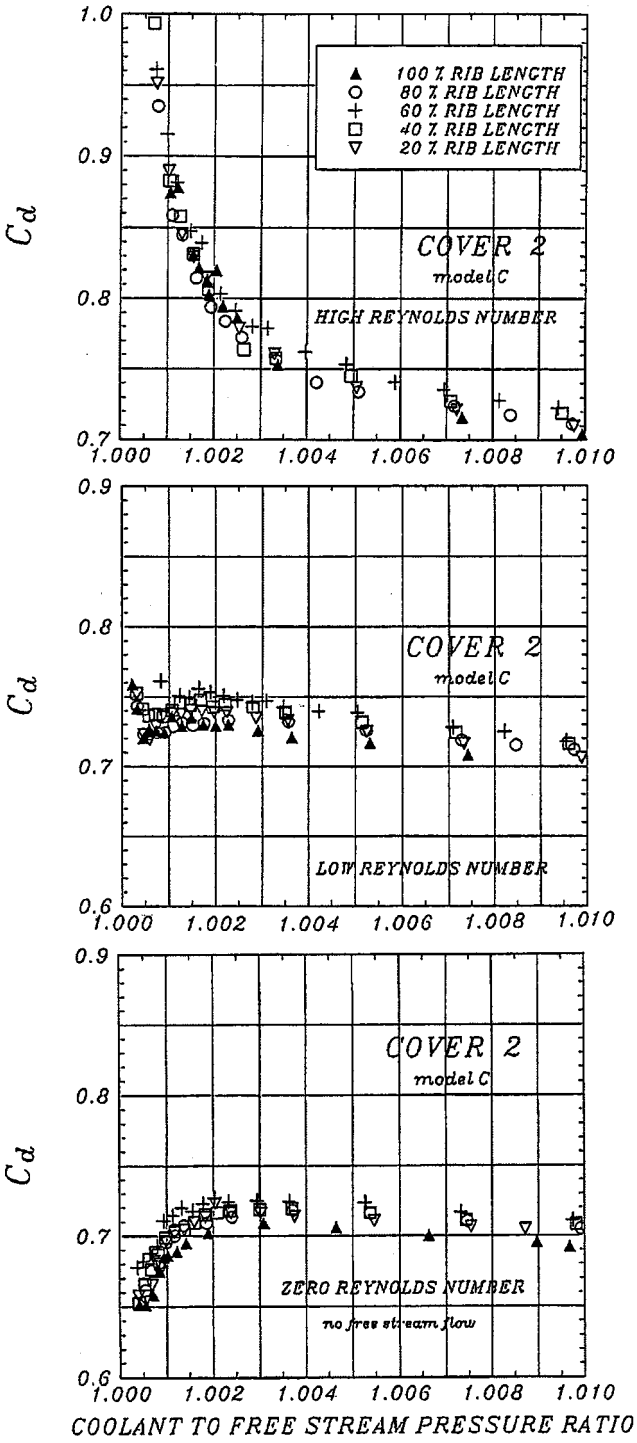

Fig. 13 Influence of rib length on discharge coefficients (Model *C*, Cover 2)

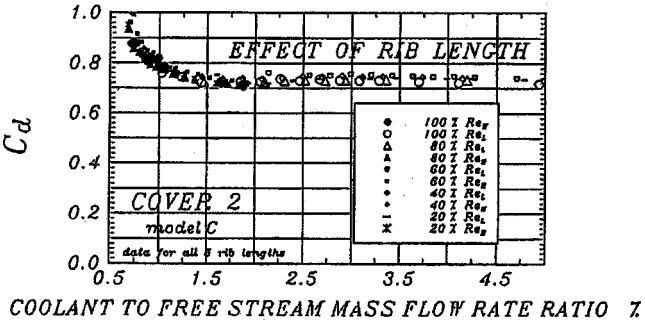

Fig. 14 Discharge coefficients versus coolant to free-stream mass flow rate ratio (model *C*, Cover 2, data for all five rib lengths)

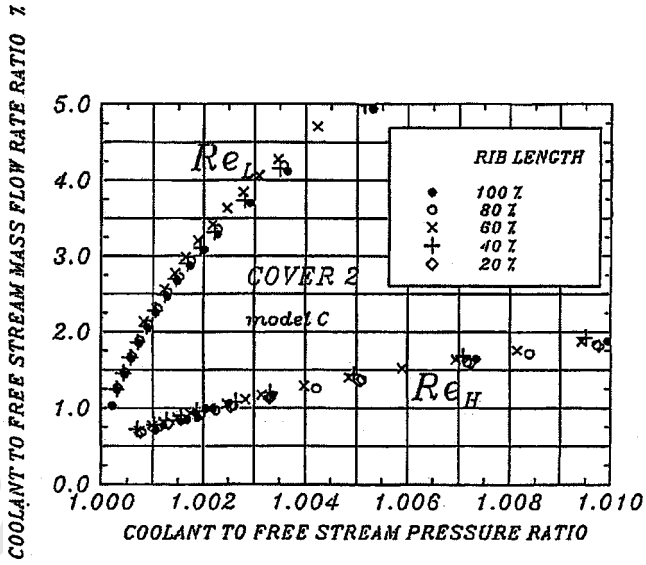

Fig. 15 Actual coolant mass flow rate versus pressure ratio (Model *C*, Cover 2, data for all five rib lengths)

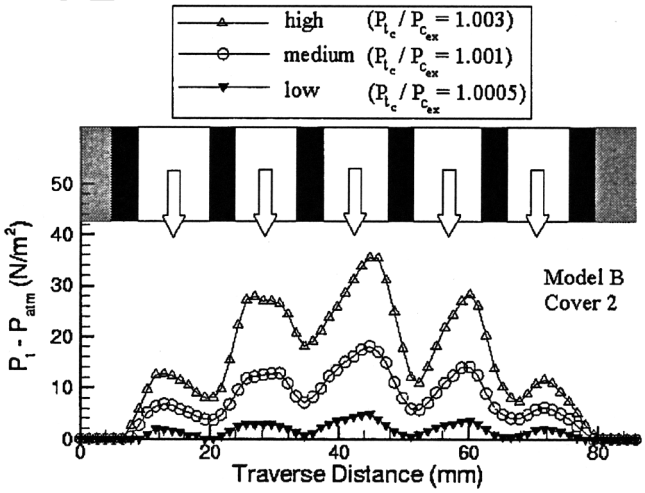

Fig. 16 Spanwise total pressure uniformity at the trailing edge

conducted for three different coolant to free-stream pressure ratios representing the mass flow range used throughout this study. The coolant is injected into a still environment in order to reveal possible spanwise nonuniformities due to internal cooling system design.

The results of the spanwise traverse are shown in Fig. 16. The coolant ejection from the trailing edge stays reasonably uniform along the span for low coolant to free-stream pressure ratios. More coolant mass flow is directed through the central channels, whereas the channels toward the sides of the ejection system can deliver less mass flow as the coolant to free-stream pressure ratio is increased. This is a natural trend for the specific coolant delivery system defined in Fig. 4. Equivalent mass flow rates introduced from the left and right side of the coolant feed pipe result in a higher coolant total pressure in the central region of the cavity.

These results indicate that the specific coolant ejection system with the copper coolant feed pipe was successful in producing a good spanwise uniformity of coolant mass flow rate.

Conclusions

An experimental study of the internal fluid mechanic loss characteristics of a turbine blade with trailing edge coolant ejection is presented. The main emphasis is placed on the determination of the discharge coefficients under realistic gas turbine conditions. The effect of cut-back length, spanwise rib spacing, free-stream Reynolds number, and chordwise rib length on discharge coefficients is studied in detail. The discharge coefficients are obtained in a wide range of coolant to free-stream mass flow rate values.

The cooling experiments were performed at three different free-stream Reynolds numbers. Discharge experiments were also conducted in still air. The discharge coefficients are presented as functions of the coolant to free-stream pressure ratio. When the C_d results are plotted against the coolant to free-stream mass flow rate ratio, the free-stream Reynolds number dependency of the data can be removed.

The C_d has a smoothly varying character at low coolant to free-stream pressure levels. However, after reaching a threshold P_{tc}/P_{cex} value, the discharge coefficients reach a constant level.

Since the discharge coefficients do not have Reynolds number dependency, C_d experiments can be performed at a low free-stream Reynolds number. Running a discharge coefficient experiment at low Reynolds number (or even in still air) will sufficiently define the high blowing rate portion of the curve. This approach is extremely time efficient and economical in finding the worst possible C_d value for a given trailing edge coolant system.

Experiments performed at three different rib spacing values show that Model *C* with 11 ribs and 10 passages is aerodynamically superior to Models *A* and *B*, which have smaller numbers of ribs and larger rib spacing.

Four different pressure side covers representing different cut-back lengths on the pressure side show that Cover 1 ($s=0.0$ mm) and Cover 2 ($s=7.8$ mm) are the two most effective cases as far as the C_d levels are concerned. Covers 3 and 4 always produced higher aerodynamic losses in the cooling system. Higher losses for this case are associated with the increasing free-stream interaction length of the wall shear layer defined after the pressure side lip.

The increased effective exit area from the coolant cavity is also responsible from the relatively lower momentum levels in the coolant jet. The discharge coefficients obtained from Covers 4 and 3 have magnitudes less than the values obtained with Covers 1 and 2.

The most successful configuration producing the highest discharge coefficients is Cover 2 with the highest number of ribs (Model *C*).

Cover 2 with Model *C* has been used for rib length experiments. Five different rib lengths ranging from 20 to 100 percent indicate that the influence of the rib length on measured aerodynamic losses is minimal. Slight variations of C_d are well within the estimated uncertainty band for the discharge coefficient.

Acknowledgments

This paper is based on a research project funded by Solar Turbines Inc. The turbine cascade used in the current study was provided by NASA Lewis (Glenn) Research Center. The authors would like to acknowledge the equipment support provided by S. A. Hippensteele and Dr. R. E. Gaugler of NASA (Glenn) Research Center, Cleveland, OH. The authors are also grateful for the equipment grant provided by the College of Engineering of the Pennsylvania State University. The grant was used for the acquisition of the PIV equipment extensively used in this study.

Nomenclature

A = effective flow area
a = spanwise rib spacing
b = spanwise rib width
c = blade chord length
C_d = discharge coefficient
h = effective channel height at exit plane (pressure side lip location)
k = turbulent kinetic energy
$\dot{m}$ = mass flow rate
$(\dot{m}_c/\dot{m}_\infty)$ = coolant to free-stream mass flow rate ratio
p = static pressure
p^* = nondimensional static pressure $(=p-p_{\text{ref}})\rho u_0{}^2$
$\text{Re}_{\max}$ = maximum Reynolds number calculated using maximum velocity at throat and blade chord
R = gas constant
RL = relative rib length (20, 40, 60, 80, and 100 percent) cut-back length measured from trailing edge point
s = cut-back length measured from trailing edge point
Tu_∞ = free-stream turbulence intensity
u = streamwise velocity
$V_{\max}$ = maximum velocity at throat
γ = specific heat ratio
δ = uncertainty of measured quantity
μ_0 = absolute viscosity
μ_t = turbulent viscosity
ρ = density

Subscripts

c = coolant
act = actual
H = high Reynolds number
is = isentropic
L = low Reynolds number
M = medium Reynolds number
0 = without mainstream flow
ex = exit reference location 3 mm downstream of trailing edge
t = total condition

References

[1] Metzger, D. E., Kim, Y. W., and Yu, Y., 1993, ''Turbine Cooling: An Overview and Some Focus Topics,'' *Proc. 1993 International Symposium on Transport Phenomena in Thermal Engineering*.
[2] McMartin, I. P., and Norbury, J. F., 1974, ''The Aerodynamics of a Turbine Cascade With Supersonic Discharge and Trailing Edge Blowing,'' ASME Paper No. 74-GT-120.
[3] Prust, H. W., 1975, ''Cold Air Study of the Effect on Turbine Stator Blade Aerodynamic Performance of Coolant Ejection from Various Trailing Edge Slot Geometries, Part II: Comparison of Experimental and Analytical Results,'' NASA Paper No. TM-X-3190.
[4] Lokai, V. I., and Kumirov, B. A., 1973, ''Losses in Turbine Cascades With Cooling Air Discharge and Various Trailing Edge Geometries,'' Izw. Vuz. Aviats. Tekn., **16**, No. 3.
[5] Lawaczek, O., 1977, ''The influence of Jets of Cooling Air Exhausted From the Trailing Edges of a Supercritical Turbine Cascade on the Aerodynamical Data,'' AGARD CP229, Paper No. 30.
[6] Sturedus, C. J., 1979, ''Aerodynamic Effects of Surface Cooling-Flow Injection on Turbine Transonic Flow Fields,'' AIAA paper No. 79-1210.
[7] Moses, H. L., Kiss, T., Bertsch, R., and Gergory, B. A. 1991, ''Aerodynamic Losses Due to Pressure Side Coolant Ejection in a Transonic Turbine Cascade,'' AIAA Paper No. 91-2032.
[8] Venediktov, V. D., 1972, ''Investigating a Turbine Stage With Cooling Air Leaving Through Slots in the Concave Surfaces of the Nozzle Blades,'' Teploenergetika, **19**, No. 7, pp. 15–19.
[9] Kiock, R., Hoheisel, H., Dietrichs, H. J., and Holmes, A. T., 1985, ''The Boundary Layer Behavior of an Advanced Gas Turbine Rotor Blade Under the Influence of Simulated Film Cooling,'' *AGARD Conf. Proc. No. 390, Heat Transfer and Cooling in Gas Turbines*, pp. 42-1–42-19.
[10] Wifert, G., and Fottner, L., 1996, ''The Aerodynamic Mixing Effect of Dis-

crete Cooling Jets With Mainstream Flow on a Highly Loaded Turbine Blade,'' ASME J. Turbomach., **118**, pp. 468–477.
[11] Gaugler, R. E., and Russell, L. M., 1980, ''Streakline Flow Visualization Study of a Horseshoe Vortex in a Large-Scale, Two-Dimensional Turbine Stator Cascade,'' ASME Paper No. 80-GT-4.
[12] Hippensteele, S. A., Russell, L. M., and Torres, F . J., 1985, ''Local Heat Transfer Measurements on a Large, Scale-Model Turbine Blade Airfoil Using a Composite of a Heater Element and Liquid Crystals,'' NASA T M 86900.
[13] Uzol, O., and Camci, C., 2000, ''Aerodynamic Loss Characteristics of a Turbine Blade With Trailing Edge Coolant Ejection: PArt 2—External Aerodynamics, Total Pressure Losses, and Predictions,'' ASME J. Turbomach., **123**, this issue, pp. ■■■–■■■.